ALKALI SULFATES WITH APHTHITALITE-LIKE STRUCTURES FROM FUMAROLES OF THE TOLBACHIK VOLCANO, KAMCHATKA, RUSSIA. I. METATHÉNARDITE, A NATURAL HIGH-TEMPERATURE MODIFICATION OF Na$_2$SO$_4$

Igor V. PEKOV[§], Nadezhda V. SHCHIPALKINA, and Natalia V. ZUBKOVA

Faculty of Geology, Moscow State University, Leninskie Gory, 119991 Moscow, Russia

Vladislav V. GURZHIY

Department of Crystallography, St. Petersburg State University, Universitetskaya Nab. 7/9, 199034 St. Petersburg, Russia

Atali A. AGAKHANOV and Dmitry I. BELAKOVSKIY

Fersman Mineralogical Museum of Russian Academy of Sciences, Leninskiy Prospekt 18-2, Moscow, 119071 Russia

Nikita V. CHUKANOV

Institute of Problems of Chemical Physics, Russian Academy of Sciences, Chernogolovka, Moscow region, 142432 Russia

Inna S. LYKOVA

Canadian Museum of Nature, 240 McLeod Street, Ottawa, Ontario K2P 2R1, Canada
Faculty of Geology, Moscow State University, Leninskie Gory, 119991 Moscow, Russia

Marina F. VIGASINA and Natalia N. KOSHLYAKOVA

Faculty of Geology, Moscow State University, Leninskie Gory, 119991 Moscow, Russia

Evgeny G. SIDOROV

Institute of Volcanology and Seismology, Far Eastern Branch of the Russian Academy of Sciences, Piip Boulevard 9, 683006 Petropavlovsk-Kamchatsky, Russia

Gerald GIESTER

Department of Mineralogy and Crystallography, University of Vienna, Althanstraße 14, 1090 Vienna, Austria

ABSTRACT

A new mineral, metathénardite, ideally Na$_2$SO$_4$, the high-temperature hexagonal dimorph of thénardite, a natural analogue of the synthetic phase Na$_2$SO$_4$(I), was found in the sublimates of active fumaroles at the Second scoria cone of the Northern Breakthrough of the Great Tolbachik Fissure eruption, Tolbachik volcano, Kamchatka, Russia. The holotype originates from the Glavnaya Tenoritovaya fumarole in which metathénardite is associated with hematite, tenorite, fluorophlogopite, sanidine, anhydrite, krasheninnikovite, vanthoffite, glauberite, johillerite, and lammerite. The cotypes 1 and 2 are from the Arsenarnaya (with hematite, tenorite, fluorophlogopite, sanidine, euchlorine, wulffite, anhydrite, fluoborite, johillerite, nickenichite, calciojohillerite, badalovite, tilasite, cassiterite, and pseudobrookite) and the Yadovitaya (with tenorite, euchlorine, fedotovite, dolerophanite, langbeinite, krasheninnikovite, anhydrite, and hematite) fumaroles, respectively. All specimens with metathénardite were collected from areas with temperatures of 350–400 °C. Metathénardite forms hexagonal tabular, lamellar, or dipyramidal crystals (forms: {001}, {100}, {102}, and {201}) up to 3 mm combined in crusts up to several hundred cm^2 in

§ *Corresponding author e-mail address*: igorpekov@mail.ru

area. The mineral is transparent to semitransparent, colorless, white, light-blue, greenish, yellowish, grayish or brownish, with vitreous luster. $D_{meas.} = 2.72(1)$, $D_{calc.} = 2.717$ g/cm^3. Metathénardite is optically uniaxial (–), $\omega = 1.489(2)$, $\varepsilon = 1.486(2)$. The empirical formulae are $(Na_{1.92}K_{0.05}Ca_{0.02}Zn_{0.01})[S_{0.99}O_4]$ (holotype), $(Na_{1.54}K_{0.22}Ca_{0.09}Cu_{0.01}Mg_{0.01})[S_{1.00}O_4]$ (cotype 1), and $Na_{1.65}K_{0.11}Ca_{0.05}Cu_{0.04}Mg_{0.01})[S_{1.01}O_4]$ (cotype 2). Admixed K and bivalent cations probably stabilize the hexagonal aphthitalite-like structure of metathénardite at room temperature. The crystal structure was solved using single crystals of all three samples, $R_1 = 0.0852$, 0.0452, and 0.0449 for holotype and cotypes 1 and 2, respectively. The space group is $P6_3/mmc$, and the unit-cell parameters of the holotype are $a = 5.3467(9)$, $c = 7.0876(16)$ Å, $V = 157.47(6)$ Å^3, and $Z = 2$. The strongest reflections of the powder X-ray diffraction pattern $[d,Å(I)(hkl)]$ are: 4.667(27)(100), 3.904(89)(101), 3.565(33)(002), 2.824(94)(102), 2.686(100)(110), and 1.939(35)(202). Metathénardite and thénardite clearly differ from one another in X-ray diffraction data and infrared and Raman spectra.

Keywords: metathénardite, new mineral, sodium sulfate, thénardite, aphthitalite group, crystal structure, fumarole, Tolbachik volcano, Kamchatka.

INTRODUCTION

Just seven years ago alkali sulfate minerals with aphthitalite-like structures were represented by only one valid species, aphthitalite, ideally $K_3Na(SO_4)_2$, which has been known in nature for more than two hundred years, being first described as "vesuvian salt" from fumarole deposits of the famous Vesuvius volcano in Italy (Smithson 1813). Besides volcanic fumaroles, aphthitalite is a typical mineral of potassium salt deposits in evaporitic rocks (Palache *et al*. 1951, Anthony *et al*. 2003).

In the structural sense, aphthitalite (also known as glaserite) became an "ancestor" of a large family of synthetic compounds which belong to different chemical classes. The general formula of numerous aphthitalite- (= glaserite-) type compounds is $^{XII}X^XY_2[^{VI}M(^{IV}TO_4)_2]$ ($Z = 1$) in which Roman numerals indicate coordination numbers. The X, Y, M, and T sites can be occupied by various atoms in more than 100 synthetic compounds: X and $Y = Na$, K, Rb, Cs, Ca, Sr, Ba, Ag, Tl, Pb, [vac]; $M = Na$, Mg, Ca, Sc, Y, Ln, Ti, Zr, Hf, V, Cr, Mo, Mn, Fe, Co, Ni, Cu, Zn, Cd, Al, In, Tl, Ge, Sn, Sb; $T = S$, Si, P, Se, V, Cr, Mo, W, Re, Fe, Ru (Lazoryak 1996, Nikolova & Kostov-Kytin 2013). The basic statements on the crystal chemistry of this family were most developed by Moore (1973, 1976, 1981).

Recent years have been marked by the explosive extension of the diversity of natural aphthitalite-related alkali sulfates. The potassium-ammonium ordered analogue of aphthitalite, the new mineral möhnite $(NH_4)K_2Na(SO_4)_2$, was described from the guano deposit at Pabellón de Pica, Iquique Province, Tarapacá, Chile (Chukanov *et al*. 2015). Four other recently discovered aphthitalite-related alkali sulfate minerals originate from active fumaroles born by the Tolbachik volcano, Kamchatka, Russia. They are (in chronological order of discovery) bubnovaite K_2Na_8 $Ca(SO_4)_6$ (IMA No. 2014–108, Gorelova *et al*. 2016),

metathénardite Na_2SO_4 (IMA No. 2015–102, Pekov *et al*. 2016), belomarinaite $KNaSO_4$ (IMA No. 2017–069a, Filatov *et al*. 2019), and natroaphthitalite $KNa_3(SO_4)_2$ (IMA No. 2018–091, Shchipalkina *et al*. 2018). Aphthitalite, möhnite, metathénardite, belomarinaite, and natroaphthitalite are hexagonal or trigonal with similar unit-cell dimensions ($a = 5.3$–5.8 and $c = 7.05$–7.45 Å) and differ from each other in composition and in distribution of cations that result in different space groups (see below). These five minerals could be united in the aphthitalite group. The trigonal sulfate bubnovaite demonstrates a more complicated scheme of cation ordering and possesses unit cell dimensions $a = 10.80$ and $c = 22.01$ Å, *i.e.*, both parameters multiplied in comparison with the minerals in the group, so its structure can be considered to be a superstructure based on the aphthitalite type (Gorelova *et al*. 2016).

Our work on aphthitalite-like alkali sulfates from Tolbachik resulted in the discoveries of two new mineral species, metathénardite and natroaphthitalite, and the obtaining of additional novel mineralogical and crystal chemical data on this mineral group. These data will be reported in this series of papers.

In the present article we describe the new mineral metathénardite (Cyrillic: метатенардит), ideally Na_2SO_4, named for its dimorphous relationship with thénardite. The name "metathénardite" was assigned in 1905 by Alfred Lacroix to a hypothetical, presumably hexagonal, unstable at room temperature, high-temperature modification of Na_2SO_4 which was observed in hot fumarolic deposits at the active Mt. Pelée volcano, Martinique, Lesser Antilles, French West Indies, and was quickly transformed to thénardite after cooling (Lacroix 1910, Palache *et al*. 1951). Later this name was applied to the synthetic hexagonal ($P6_3/mmc$) phase $Na_2SO_4(I)$, a well-studied artificial analogue of the mineral described here. We decided to keep this historical name.

Both the new mineral and its name have been approved by the Commission on New Minerals, Nomenclature and Classification of the International Mineralogical Association (IMA CNMNC). The type specimens of metathénardite are deposited in the systematic collection of the Fersman Mineralogical Museum of the Russian Academy of Sciences, Moscow, with the catalogue numbers 95281 (the holotype) and 95590.

Background Information: Brief Data on the System Na₂SO₄–K₂SO₄ and Crystal Structure of Hexagonal Na₂SO₄

Phases in the Na_2SO_4–K_2SO_4 system

The synthetic system Na_2SO_4–K_2SO_4 is, in general, well-studied. The phase transitions, characteristics of some crystal structures, phase relations, and thermodynamic stability fields of several phases in this system have been reported (Kracek & Ksanda 1930, Hilmy 1953, Eysel 1973, Okada & Ossaka 1980, Dessureault *et al*. 1990, Du 2000 and references therein).

Five polymorphs of Na_2SO_4 are known among synthetic compounds; they are traditionally labelled as phases Na_2SO_4(I, II, III, IV, V). A natural analogue and valid mineral species was only previously known for the room-temperature modification Na_2SO_4(V); this was orthorhombic (*Fddd*) thénardite. The pattern of phase transitions in this system is complicated, and many publications report on the thermal behavior of Na_2SO_4. Reviews of the crystal structures and phase transitions for its polymorphs are given by Kumari & Secco (1983), Eysel *et al*. (1985), and Rasmussen *et al*. (1996). According to experimental data, the aphthitalite-related hexagonal phase Na_2SO_4(I) (space group $P6_3/mmc$) is stable above 240 °C. Below 240 °C this phase transforms to Na_2SO_4(II) (orthorhombic, *Pbnm*). The phase transition II–III happens after cooling up to 219 °C. The phase Na_2SO_4(III) (orthorhombic, *Cmcm*) can be directly and irreversibly transformed into Na_2SO_4(I) by heating at 241 °C. The modification Na_2SO_4(IV) can coexist with Na_2SO_4(III) in the range 209–219 °C. Na_2SO_4(V), corresponding to thénardite, is stable under 186 °C (Nord 1973). Metathénardite is the natural analogue of Na_2SO_4(I); see below.

The phases with aphthitalite *sensu stricto* structure (trigonal, $P\bar{3}m1$) and related KNaSO₄ structure (trigonal, $P3m1$) can form below 470 °C in the subsolidus region (Du 2000). The compositional field of these phases is wide and involves compounds with the K:Na ratio varying from 1:3 to 3:1, *i.e.*, with compositions between $KNa_3(SO_4)_2$ and $K_3Na(SO_4)_2$. Three individual synthetic phases have been described in this series: $K_3Na(SO_4)_2$ ($P\bar{3}m1$), KNaSO₄ ($P3m1$),

and $KNa_3(SO_4)_2$ ($P\bar{3}m1$) (Bellanca 1942, Hilmy 1953, Eysel 1970, 1972, 1973, Okada & Ossaka 1980 and references therein). Aphthitalite ($P\bar{3}m1$) (Fischmeister 1962), belomarinaite ($P3m1$) (Filatov *et al*. 2019), and natroaphthitalite ($P\bar{3}m1$) (Shchipalkina *et al*. 2018), respectively, are the natural analogues of these synthetic sulfates. This part of the solid-solution system will be discussed in the next article of the present series.

Two polymorphs of K_2SO_4 are known. Synthetic K_2SO_4(I) (hexagonal, $P6_3/mmc$), existing above 583 °C (Berg & Tunistra 1978, Miyake *et al*. 1980), is a structural analogue of synthetic Na_2SO_4(I) (metathénardite). K_2SO_4(II) is a low-temperature modification (orthorhombic, *Pnma*) stable below 583 °C to room temperature (Hilmy 1953). In nature it is the mineral arcanite, which was structurally characterized by Zubkova *et al*. (2018) using a specimen from Tolbachik.

Crystal structure of Na_2SO_4(I)

The crystal structure of synthetic hexagonal ($P6_3/mmc$) Na_2SO_4(I) (Fig. 1), an analogue of the endmember metathénardite, is well studied (Fischmeister 1962, Eysel *et al*. 1985, Naruse *et al*. 1987, Rasmussen *et al*. 1996). The unit cell contains four Na cations and two SO₄ tetrahedra. The Na cations are located at high-symmetry sites $3m$ and $6m2$ and the tetrahedrally coordinated S atom at $6m2$, whereas the O atoms are placed at $.m.$ and $m..$ planes, resulting in 12 partially occupied O positions coordinating S.

Despite the apparent simplicity, this crystal structure was controversial because of complicated disorder that led to conflicting results in the literature (Eysel *et al*. 1985). The disorder is due to various orientations of SO₄ tetrahedra (Fig. 2): «up-down», «tilting», «left-right», and a combination of «up-down» and «tilting» disorder. All of these types have been discussed in detail (Eysel *et al*. 1985 and references therein). The presence of such disorder makes it impossible to correctly define the coordination polyhedra for two Na atoms. However, in some publications, for Na in the crystal structure of Na_2SO_4(I) two different polyhedra are reported: for Na1 a 10-fold polyhedron with four close (2.52 Å), two intermediate (2.80 Å), and four distant (3.00 Å) O neighbors and for Na2 six close O atoms (2.31–2.40 Å) (Eysel *et al*. 1985, Naruse *et al*. 1987).

Metathénardite: Type Specimens, Occurrence, and General Appearance

The specimen which became the holotype of metathénardite was found by us in July 2012 in the
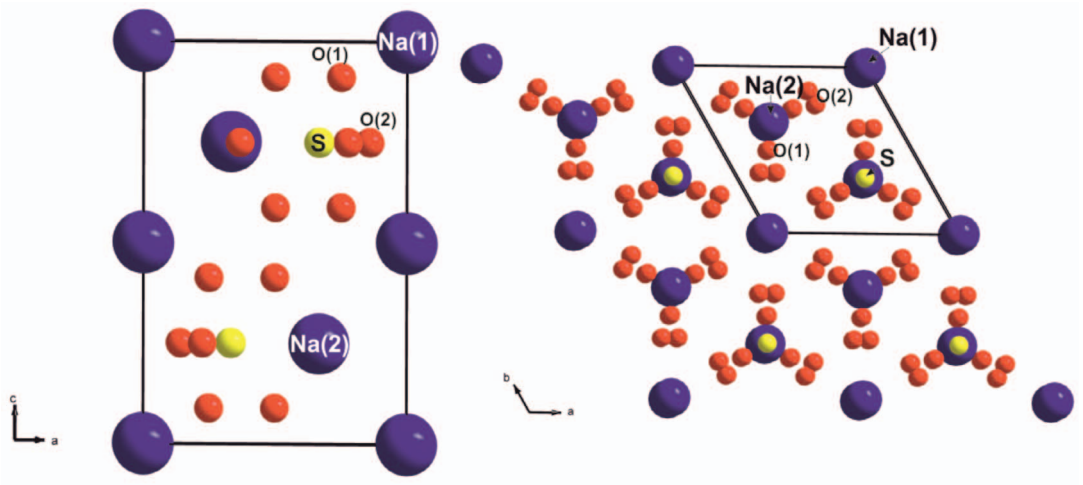
FIG. 1. Projections of the crystal structure of metathénardite [= Na₂SO₄(I)] along the **b** axis (left) and the **c** axis (right). The occupancy of each O site is 1/3. The unit cell is outlined.
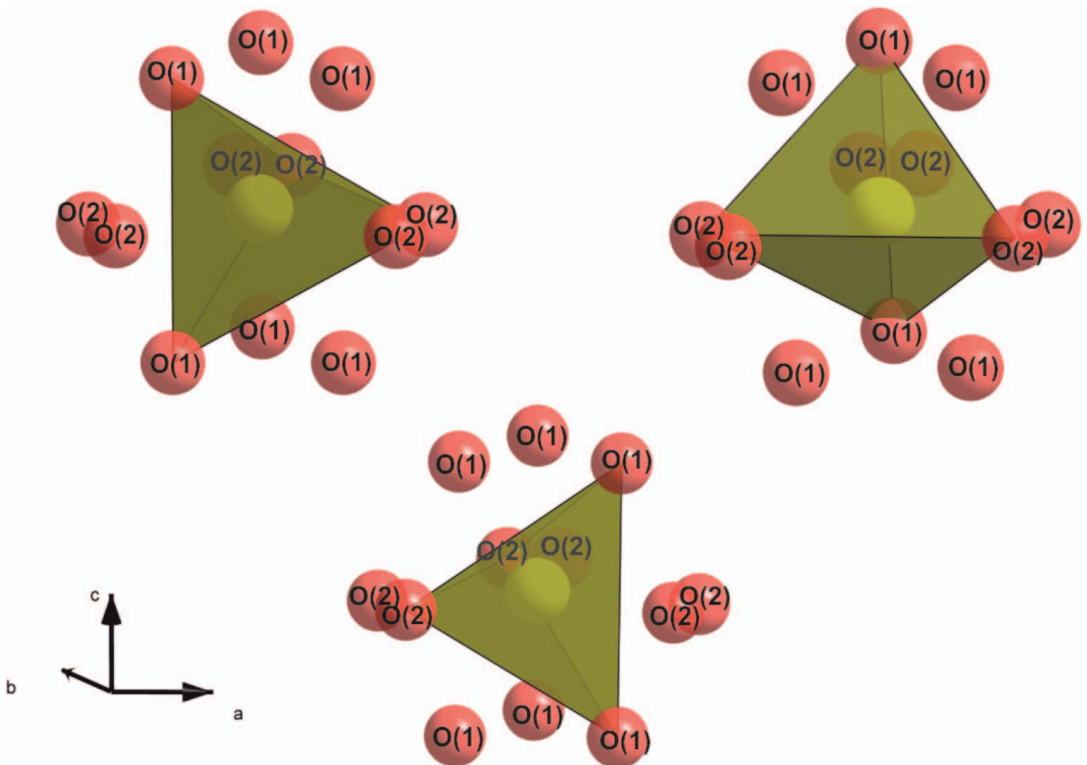

FIG. 2. Types of orientation of the SO₄ tetrahedron in the crystal structure of metathénardite (the holotype) [= Na₂SO₄(I)] along the **b** axis. The occupancy of each O site is 1/3.

Glavnaya Tenoritovaya ("Major Tenorite") fumarole at the summit of the Second scoria cone of the Northern Breakthrough of the Great Tolbachik Fissure Eruption (NB GTFE), Tolbachik volcano, Kamchatka Peninsula, Far-Eastern Region, Russia (55°41′N 160°14′E, 1200 m asl). The first study of the mineral, including crystal structure determination, was carried out using this holotype specimen, and metathénardite was approved by the IMA CNMNC as a new species based on that description (Pekov *et al.* 2016). Later the mineral was identified by us in several other Tolbachik fumaroles. We discovered that (1) metathénardite is a common sulfate mineral in high-temperature exhalations of three active fumaroles located at the apical part of the Second scoria cone of the NB GTFE, namely Glavnaya Tenoritovaya, Yadovitaya ("Poisonous"), and Arsenatnaya and (2) metathénardite is represented by several varieties which distinctly differ from each other in some chemical and structural features. The present paper contains, besides data for the holotype from Glavnaya Tenoritovaya, data for metathénardite samples from the Yadovitaya and Arsenatnaya fumaroles that are considered to be cotypes.

The Second scoria cone of the NB GTFE is a monogenetic volcano about 300 m high and approximately 0.1 km^3 in volume formed in 1975. It is situated 18 km SSW of the active volcano Ploskiy Tolbachik (Fedotov & Markhinin 1983) and demonstrates strong fumarolic activity to the present day. General descriptions of the fumaroles in which metathénardite was identified are given in the following papers: Glavnaya Tenoritovaya was described by Pekov *et al.* (2015), Yadovitaya by Vergasova & Filatov (2016), and Arsenatnaya by Pekov *et al.* (2018).

Specimens with metathénardite were collected from hot zones of all three fumaroles. The temperatures in these areas (inside cracks and cavities immediately after their uncovering) measured by us using a chromel-alumel thermocouple varied from 350 to 400 °C.

Specimen #3694 (the holotype) originates from the Glavnaya Tenoritovaya fumarole, where metathénardite is associated with hematite, tenorite, fluorophlogopite, sanidine, anhydrite, krasheninnikovite, vanthoffite, glauberite, johillerite, and lammerite. The secondary, supergene association includes gypsum, blödite, and powdery aggregates of unidentified sulfates of Na, K, Ca, and Mg. At this location the metathénardite occurs as interrupted crusts up to 2 × 2 cm^2 in area and up to 0.2 mm thick overgrowing basalt scoria or thin incrustations of fluorophlogopite and hematite covering the surface of basalt scoria. The metathénardite crusts typically consist of irregularly shaped grains or coarse, flattened, lens-shaped crystals (Fig. 3a) up to 0.1 mm across. Rarely, well-formed dipyramidal crystals (up to 0.07 mm) combined in clusters or crusts (Fig. 4a) are observed. They are formed by faces of the hexagonal dipyramid {102} (Fig. 5a) and are typically distorted and cavernous, sometimes skeletal, with uneven surfaces (Fig. 4a, b). The crystals and grains of metathénardite usually have mosaic, blocky inner structure (with single-crystal blocks up to 15 μm, rarely up to 10 × 25 μm^2) and commonly contain abundant dust-like inclusions of hematite.

Specimen #4089 (the cotype 1) was collected in July 2013 from the Arsenatnaya fumarole. The typical associated minerals are hematite, tenorite, fluorophlogopite, sanidine, euchlorine, wulffite, anhydrite, fluoborite, johillerite, nickenichite, calciojohillerite, badalovite, tilasite, cassiterite, and pseudobrookite. At this locality the metathénardite forms abundant crystal crusts and brushes (up to several hundred cm^2 in area), typically open-work, in cavities between blocks of basalt scoria and volcanic bombs at depths of 0.5–2 m from the surface. The crystals (up to 3 mm across and up to 1 mm thick) are hexagonal tabular to lamellar. They are formed by faces of the pinacoid {001} (usually the major form), the hexagonal prism {100}, and the hexagonal dipyramid {102}; narrow faces of the hexagonal dipyramid {201} were observed on some crystals (Figs. 3b, 4b, and 5b–d). Parallel or near-parallel aggregates of metathénardite crystals are common (Fig. 3b). Intergrowths with other aphthitalite-like alkali sulfates are typical for many crystals of metathénardite from Arsenatnaya, and this will be described and discussed in the next paper of the present series.

Specimen #4598 (the cotype 2) was collected in July 2015 from the southern part of the Yadovitaya fumarole. At this location metathénardite is associated with tenorite, euchlorine, fedotovite, dolerophanite, langbeinite, krasheninnikovite, anhydrite, and hematite. Metathénardite here is a widespread mineral forming clusters, incrustations, and brushes (up to 20 cm^2 in area) of hexagonal tabular crystals (Fig. 3c) up to 2 mm across and 0.5 mm thick. In morphology they are similar to the above-described crystals from Arsenatnaya. The most typical shape of metathénardite crystals from Yadovitaya is shown in Figure 5b.

PHYSICAL PROPERTIES AND OPTICAL CHARACTERISTICS

Metathénardite is transparent to semitransparent (Fig. 3), colorless, white, light-blue, greenish, yellowish, grayish, or brownish. The streak is white. The luster is vitreous. The mineral is brittle. The Mohs'
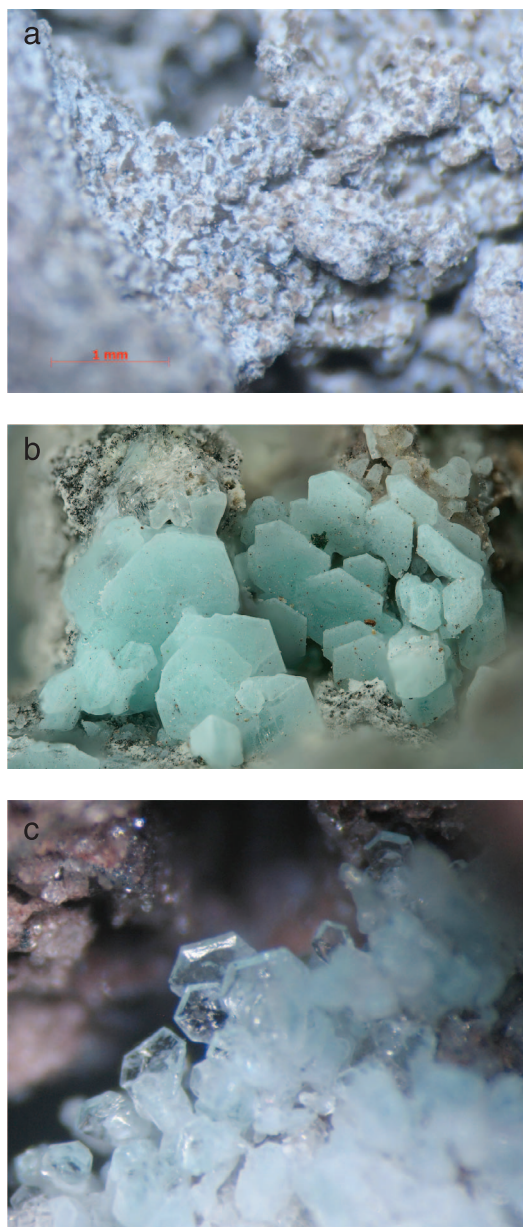
FIG. 3. Metathénardite aggregates overgrowing basalt scoria: (a) interrupted crust consisting of grayish to brownish grains partially covered by white to bluish powdery films of secondary sulfates from the Glavnaya Tenoritovaya fumarole (the holotype); (b) near-parallel groups of light blue lamellar crystals from the Arsenatnaya fumarole; (c) cluster of transparent bluish tabular crystals from the Yadovitaya fumarole (the cotype 2). FOV width: (a) 4.5 mm, (b) 3 mm, (c) 2.5 mm. Photographers: (a, c) I.V. Pekov and A.V. Kasatkin, (b) S. Wolfsried.

hardness is *ca*. 3. Cleavage or parting was not observed, and the fracture is uneven. The density of the holotype as measured by flotation in heavy liquids (bromoform + hexane) is 2.72(1) g/cm^3. The density calculated using the empirical formula of the holotype is 2.717 g/cm^3.

Metathénardite is optically uniaxial (–), with ω = 1.489(2) and ε = 1.486(2) (589 nm, data for the holotype). In transmitted plane-polarized light the mineral is colorless and non-pleochroic.

INFRARED AND RAMAN SPECTROSCOPY

The infrared (IR) absorption spectrum of a transparent, homogeneous crystal from the Yadovitaya fumarole (the cotype 2, specimen #4598) (Fig. 6a) was obtained using an ALPHA FTIR spectrometer (Bruker Optics) at a resolution of 4 cm^{-1} and 16 scans. Prior to analysis the crystal was powdered, mixed with anhydrous KBr, and pelletized (the ratio sample:KBr was 1:150 in mass proportion). The IR spectrum of an analogous pellet of pure KBr was used as a reference.

Absorption bands in the IR spectrum of metathénardite and their assignments (cm^{-1}; s – strong band, w – weak band, sh – shoulder) are: 1150sh, 1136s, 1115sh [asymmetric stretching vibrations of SO_4^{2-}, the $F_2(\nu_3)$ mode]; 993, 970sh [symmetric stretching vibrations of SO_4^{2-}, the $A_1(\nu_1)$ mode]; 630sh, 618s [bending vibrations of SO_4^{2-}, the $F_2(\nu_4)$ mode]; 490 [bending vibrations of SO_4^{2-}, the $E(\nu_2)$ mode]. The weak band at 2125 cm^{-1} may correspond to a combination mode. Two nondegenerate bands of symmetric S–O stretching vibrations (at 970 and 993 cm^{-1}) indicate that at least two distorted SO_4 tetrahedra occur in the crystal structure of metathénardite. Nondegenerate symmetric S–O stretching vibrations bands are not evident in the thénardite IR spectrum (Fig. 6b). Another feature of metathénardite distinguishing it from thénardite is the absence of a well-resolved doublet in the range 610–640 cm^{-1} because of overlapping of numerous poorly resolved bands related to different local situations around SO_4^{2-} groups.

The Raman spectrum of the holotype specimen of metathénardite (Fig. 7a) was acquired from a polycrystalline sample using an EnSpectr R532 spectrometer with a green laser (532 nm) at room temperature. The power of the laser beam on the sample was about 7 mW and the diameter of the focal spot on the sample was about 10 μm. The spectrum was processed using the EnSpectr expert mode program in the range 100 to 4000 cm^{-1} with the use of a holographic diffraction grating with 1800 lines cm^{-1} and a resolution equal to 5–8 cm^{-1}.
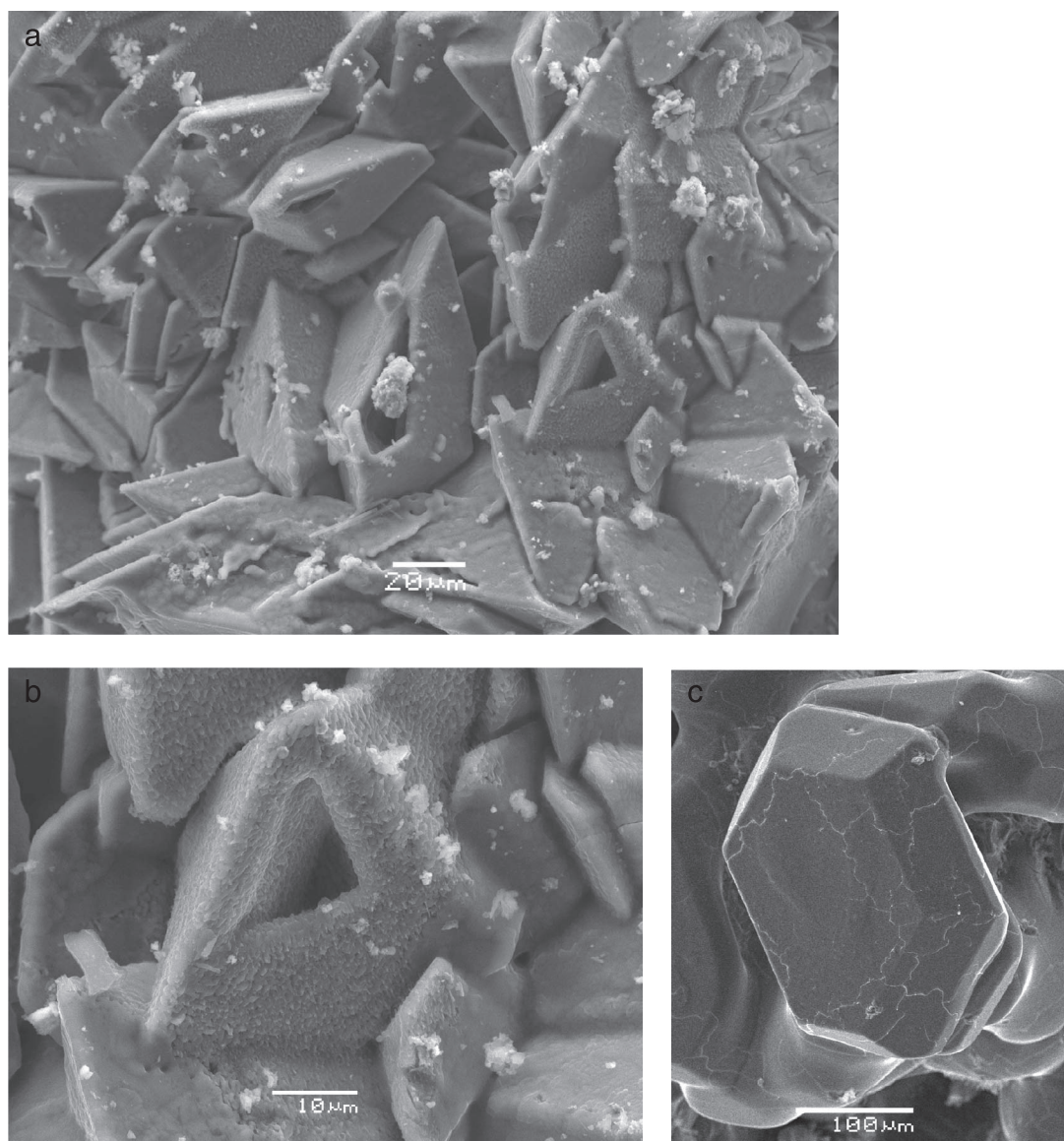
FIG. 4. Metathénardite crystals and aggregates: (a, b) crust consisting of hexagonal dipyramidal crystals (b – enlarged fragment) from the Glavnaya Tenoritovaya fumarole (the holotype), (c) typical crystal from the Arsenatnaya fumarole. SEM images, SE mode.

Bands in the Raman spectrum of metathénardite and their assignments, according to Nakamoto (1986), are (cm^{-1}, s – strong band): 1169, 1103 [$F_2(\nu_3)$-type stretching vibrations of SO$_4^{2-}$]; 1016s [$A_1(\nu_1)$ symmetric stretching vibrations of SO$_4^{2-}$]; 684, 638 [$F_2(\nu_4)$ bending vibrations of SO$_4^{2-}$]; 485, 450 [$E(\nu_2)$ bending vibrations of SO$_4^{2-}$]. The Raman spectrum of the synthetic analogue of metathénardite, a hexagonal phase Na$_2$SO$_4$ (I) (Cody *et al.* 1981), is similar.

The Raman spectra of metathénardite and thénardite (Fig. 7b) have some common features but differ significantly from one another in number of bands and their positions (wavenumbers).

The lack of bands with frequencies higher than 1200 cm^{-1} in both IR and Raman spectra of metathénardite indicates the absence of groups with O–H, C–H, C–O, N–H, and N–O bonds in the mineral.
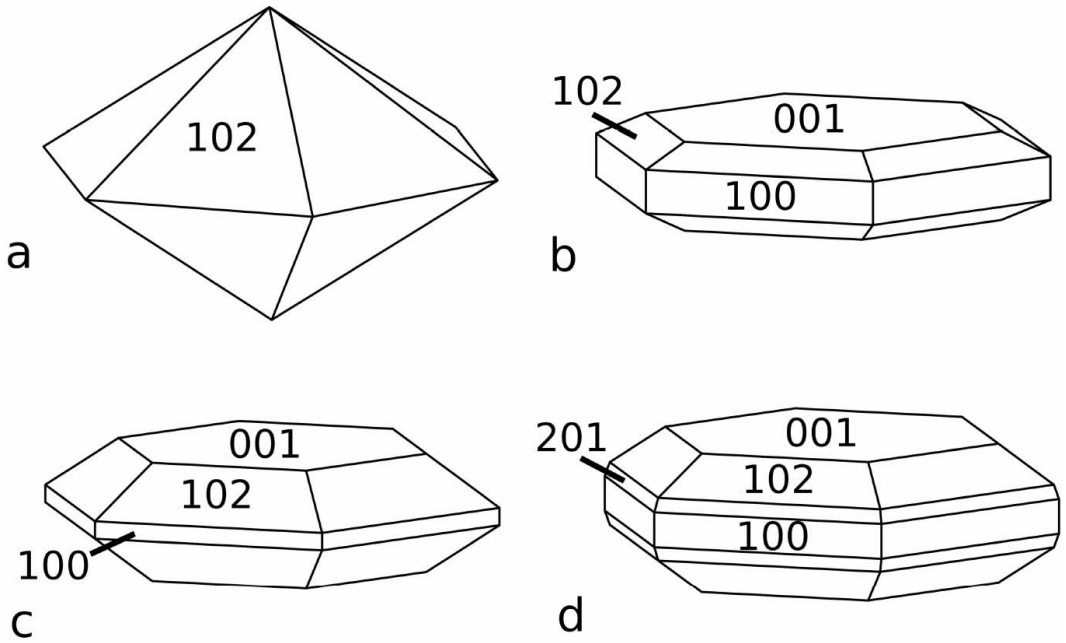
FIG. 5. Crystals of metathénardite from (a) Glavnaya Tenoritovaya and (b–d) Arsenatnaya and Yadovitaya fumaroles, Tolbachik volcano.
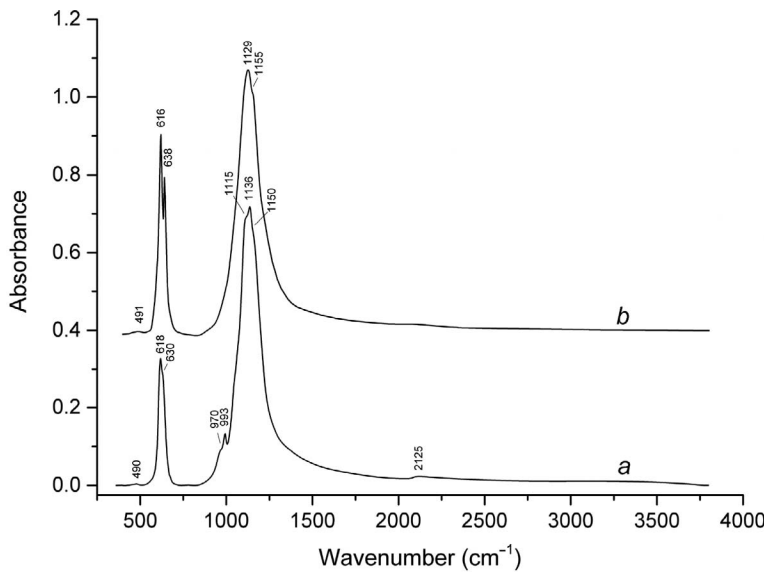

FIG. 6. The IR spectra of (a) metathénardite (cotype 2) and (b) thénardite from Searles Lake, California, USA. The spectra are offset for comparison.
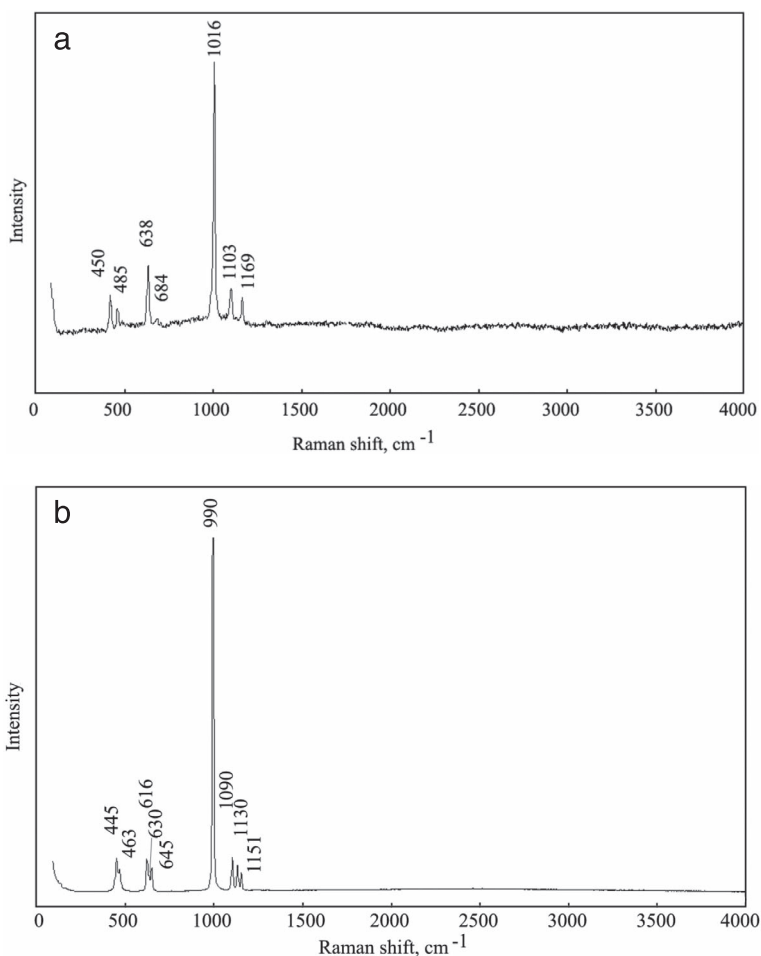
FIG. 7. The Raman spectra of the (a) holotype metathénardite and (b) thénardite from the Chumyshkul' lake, Aralsk district, Kazakhstan.

CHEMICAL DATA

The chemical composition of metathénardite was studied by electron microprobe in two laboratories. In the Fersman Mineralogical Museum of the Russian Academy of Sciences (FMM) the holotype specimen was studied using a Jeol 733 electron microprobe instrument. In the Laboratory of Analytical Techniques of High Spatial Resolution in the Department of Petrology of Moscow State University (MSU) the chemical composition of both cotype specimens was determined using a Jeol JSM-6480LV scanning electron microscope equipped with an INCA-Wave 500 wavelength-dispersive spectrometer. In both laboratories the analyses were carried out using WDS mode, with an acceleration voltage of 20 kV, a beam current of 10 nA, and a beam diameter of 3 μm.

The following reference materials were used (FMM / MSU): Na: omphacite / NaCl; K: microcline / potassic feldspar; Ca: anorthite / wollastonite; Mn: none / Mn; Zn: ZnS / ZnS; Cu: none / Cu; S: $BaSO_4$ / FeS_2. Contents of other elements with atomic numbers higher than carbon are below detection limit. Special attention was paid to the correctness of the determination of Na, to avoid possible overlap of analytical lines of Na and admixed Zn. For the Zn measurement, the Zn$K\alpha$1 line was used.

The chemical data for metathénardite are given in Table 1. All three studied samples are characterized by the presence, besides the species-defining cation Na, of significant contents of admixed metal cations. The major admixtures (in wt.%) are: K_2O 1.3–8.1, CaO 0.2–4.0, ZnO 0.0–2.2, and CuO 0.0–2.1. The total amount of admixed cations varies from 0.08 atoms per

TABLE 1. CHEMICAL COMPOSITION OF METATHÉNARDITE

No.	1	2	3	4
Sample no.	3694 (holotype)	4089 (cotype 1)	4598 (cotype 2)	
Na_2O (wt.%)	41.20 (40.11–42.31)	32.85 (31.04–34.56)	35.42 (35.15–35.63)	43.64
K_2O	1.57 (1.29–1.91)	7.04 (5.66–8.07)	3.53 (2.61–4.18)	
CaO	0.82 (0.21–1.54)	3.62 (2.98–3.98)	1.86 (1.63–2.06)	
MgO	-	0.18 (0.14–0.24)	0.14 (0.10–0.18)	
MnO	-	0.18 (0.11–0.25)	0.15 (0.11–0.18)	
CuO	-	0.51 (0.28–0.80)	2.07 (1.87–2.34)	
ZnO	0.66 (0.00–2.16)	0.17 (0.10–0.30)	0.23 (0.15–0.30)	
SO_3	55.01 (53.37–55.98)	55.13 (54.15–56.14)	55.76 (55.79–55.8)	56.36
Total	99.26	99.68	99.16	100.00
Formula calculated on the basis of 4 O atoms per formula unit				
Na	1.923	1.540	1.651	2
K	0.048	0.217	0.108	
Ca	0.021	0.094	0.048	
Mg	-	0.006	0.005	
Mn	-	0.004	0.003	
Cu	-	0.009	0.038	
Zn	0.012	0.003	0.004	
S	0.994	1.002	1.007	1
ΣMe	2.004	1.873	1.858	2

Note: 1, 2, and 3 – average data for 11, 11, and 16 spot analyses, respectively, ranges are in parentheses; 4 – calculated values for ideal Na_2SO_4 composition. ΣMe – sum of metal cations. Dash means the content is below detection limit.

formula unit (*apfu*, for formula calculated on the basis of 4 O atoms) in the holotype to 0.33 *apfu* in the cotype 1. The incorporation of significant amounts of admixed bivalent cations results in decreases in the total amount of metal cations to 1.87 *apfu* in cotype 1 and 1.86 *apfu* in cotype 2 (Table 1).

Metathénardite dissolves in H_2O at room temperature.

The Gladstone-Dale compatibility index (Mandarino 1981) for the holotype is $1 - (K_p/K_c) = 0.018$, superior (with both measured and calculated density values).

X-Ray Crystallography and Crystal Structure

Powder X-ray diffraction (XRD) data for the holotype specimen of metathénardite (Table 2) were collected with a STOE IPDS II diffractometer equipped with an Image Plate area detector, using the Gandolfi method (Mo$K\alpha$-radiation; detector-to-sample distance: 200 mm). The parameters of the hexagonal unit cell refined from the powder data are $a = 5.358(2)$, $c = 7.144(7)$ Å, and $V = 177.6(3)$ Å^3. Powder XRD patterns of both cotypes are very similar to that of the holotype.

Single-crystal XRD studies were carried out in two laboratories. The holotype was studied in the X-Ray Diffraction Resource Center of the St. Petersburg State University using a Bruker Kappa Duo diffractometer equipped with an Apex II CCD detector. Single-crystal XRD data for both cotype samples were collected in a full sphere of the reciprocal space with a Bruker Kappa X8 APEX diffractometer equipped with a CCD detector at the University of Vienna. The crystal structure of the holotype was refined using the SHELX program (Sheldrick 2007). The crystal structures of the cotype samples were refined with the JANA program package (Petříček *et al.* 2014). Single-crystal data, data collection information, and structure refinement details for these samples are given in Table 3.

The crystal structure of the holotype specimen of metathénardite was refined using the structure model of synthetic $Na_2SO_4(I)$ reported by Rasmussen *et al.* (1996). The structure of the mineral is just the same as of the synthetic phase described above: see *Crystal structure of $Na_2SO_4(I)$*.

The crystal structures of the cotypes were refined based on the model of the holotype. During the refinement of these structures the main challenge was to correctly determine the locations of the oxygen atoms. The extremely high anisotropic displacement parameter U_{33} for the O(1) atom [0.24(2) Å^2 and 0.24(3) Å^2 for samples 4089 and 4598, respectively], along with calculations of difference Fourier synthesis maps after refinement cycles with O(1) and O(2) atoms at special .*m*. and *m*.. positions, suggested splitting the

TABLE 2. POWDER X-RAY DIFFRACTION DATA FOR METATHÉNARDITE (THE HOLOTYPE SAMPLE)
AND ITS SYNTHETIC ANALOGUE Na$_2$SO$_4$(I)

Metathénardite				Synthetic Na$_2$SO$_4$(I)				
I_{obs}	d_{obs}	I_{calc}	d_{calc}*	I_{obs}**	d_{obs}**	I_{calc}***	d_{calc}***	hkl
27	**4.667**	15	4.630	20	4.71	1	4.612	100
89	**3.904**	77	3.876	100	3.94	100	3.872	101
33	**3.565**	29	3.544	30	3.61	78	3.563	002
94	**2.824**	70	2.814	90	2.865	74	2.820	102
100	**2.686**	100	2.673	90	2.703	68	2.663	110
12	2.325	8	2.315	20	2.346	7	2.306	200
10	2.203	6	2.201	20	2.226	12	2.194	201
		1	2.134	3	2.166	2	2.133	112
2	2.105	1	2.104	3	2.145	3	2.112	103
35	**1.939**	38	1.938	30	1.966	40	1.936	202
6	1.781	9	1.772	10	1.809	12	1.782	004
6	1.698	2	1.699	2	1.722	3	1.694	211
7	1.570	13	1.569	20	1.592	10	1.566	212
9	1.553	12	1.543	15	1.563	5	1.537	300
4	1.504	1	1.508	15	1.505	7	1.481	114
2	1.422	2	1.415	3	1.436	0.5	1.412	302
3	1.412	2	1.406	3	1.429	1	1.405	213
6	1.341	10	1.337	10	1.354	5	1.332	220
3	1.256	2, 4	1.264, 1.251	8	1.269	0.7, 2	1.259, 1.247	311, 222
2	1.207	5	1.207			2	1.204	312
2	1.167	4	1.164			2	1.164	304

* For the unit-cell parameters calculated from single-crystal data (holotype, Table 3); ** Eysel (1973) (reported in JCPDS-ICDD, #27-791); *** Eysel *et al.* (1985) (reported in JCPDS-ICDD, #78-1883). The strongest reflections of metathénardite are marked in bold.

O(1) site (Fig. 8). Splitting of the O(1) site to O(1) and O(1)' decreased the equivalent displacement parameters for these subsites to 0.0799(12) Å^2 (sample 4089) and 0.099(11) Å^2 (sample 4598). The equivalent displacement parameters were refined to be equal for subsites O1 and O1'. Thus, in these crystal structures there are two types of oxygen sites: O(1) and O(1)' subsites, which appear because of the displacement of the O(1) atom from .*m*. to general sites. All oxygen sites are substantially vacant: O(2) is 1/3 occupied and both O(1) and O(1)' are 1/6 occupied. Coordinates of atoms for all three studied samples of metathénardite are given in Table 4.

Interatomic distances for SO$_4$ tetrahedra are (in Å) as follows: holotype: 1.39(1)–1.412(16) (mean 1.40); cotype 1: 1.39(1)–1.57(1) (mean 1.50); cotype 2: 1.42(1)–1.56(1) (mean 1.49). Interatomic distances in Na-centered polyhedra are shown in Figure 9.

DISCUSSION

In terms of crystal structure, metathénardite, as well as synthetic Na$_2$SO$_4$(I), is similar to aphthitalite K$_3$Na(SO$_4$)$_2$ (Gossner 1928, Okada & Ossaka 1980). Rasmussen *et al.* (1996) also pointed out that there is a supergroup-subgroup relationship between the Na$_2$SO$_4$(I, II, III) phases. Both Na$_2$SO$_4$(II) and Na$_2$SO$_4$(III) are orthorhombic, and they crystallize in space groups *Cmcm* (III), a subgroup of *P*6$_3$/*mmc* (I), and *Pbnm* (II), a subgroup of *Cmcm*. The arrangements of Na and S are similar in these three modifications of Na$_2$SO$_4$. Unlike them, thénardite, as well as its synthetic analogue Na$_2$SO$_4$(V), is orthorhombic, *Fddd* (Nord 1973, Hawthorne & Ferguson 1975, Rasmussen *et al.* 1996), and it strongly differs in terms of structure from metathénardite and the synthetic phases Na$_2$SO$_4$(I, II, III). Table 5 demonstrates that metathénardite and thénardite are quite different minerals not only in symmetry and unit-cell dimensions, but also with respect to powder XRD patterns and optical data. In particular, these two minerals can be easily distinguished using a characteristic region in the powder XRD diagram, with *d* spacings between 3.7 and 3.0 Å: the metathénardite pattern here contains only one reflection (strong) with a *d* value about 3.6 Å, whereas thénardite demonstrates two reflections (both strong) with *d* values about 3.18 and 3.08 Å.

The unit-cell parameters of the three studied samples of metathénardite vary as follows: *a* =

TABLE 3. CRYSTAL DATA AND REFINEMENT DETAILS FOR THE HOLOTYPE AND
THE COTYPE SAMPLES OF METATHÉNARDITE

Sample	3694 (holotype)	4089 (cotype 1)	4598 (cotype 2)
Empirical formula	$(Na_{1.92}K_{0.05}Ca_{0.02}Zn_{0.01})[S_{0.99}O_4]$	$(Na_{1.54}K_{0.22}Ca_{0.09}Cu_{0.01}Mg_{0.01})[S_{1.00}O_4]$	$(Na_{1.65}K_{0.11}Ca_{0.05}Cu_{0.04}Mg_{0.01})[S_{1.01}O_4]$
Absorption, μ (mm^{-1})	1.032	1.399	1.425
D(calc.), g/cm^3	2.732	2.661	2.685
Crystal system	Hexagonal		
Space group	$P6_3/mmc$		
Unit-cell parameters			
a (Å)	5.3467(9)	5.3992(2)	5.36910(10)
c (Å)	7.0876(16)	7.1618(3)	7.1281(2)
V (Å^3)	175.47(6)	180.80(1)	177.954(7)
Z	2		
Radiation; wavelength (Å)	MoKα, 0.71069		
Data collection method	ω		
Temperature (K)	293		
F(000)	142	136	135
θ range for data (°)	4.40–28.17	4.36–30.2	4.38–30.73
Index ranges	−7< h <6, −6 < k <7, −9 < l <9	−7 < h <7, −7 < k <7, −10 < l <10	
Reflections/unique	1240/104	2661/95	3061/108
Observed reflections	102	75	99
R_{int}	5.51	3.47	3.67
Refinement method	Full-matrix least-squares on F^2		
Weighting scheme	$w = 1/[\sigma^2(Fo^2) + (0.0000P)^2 + 2.0254P]$, where $P = ([max\ of\ (0\ or\ Fo^2)] + 2Fc^2)/3$	$w = 1/(\sigma^2(I) + 0.0100000007I^2)$	$w = 1/(\sigma^2(I) + 0.0143999998I^2)$
Goodness-of-fit on F	1.34	1.00	1.00
Final R indices (%)	$R_1 = 8.52$, $wR_2 = 14.07$	$R_1 = 4.52$, $wR_2 = 11.39$	$R_1 = 4.49$, $wR_2 = 12.94$
$\Delta\rho$max /$\Delta\rho$min	0.52/–0.46	0.42/–0.62	0.30/–0.27

5.347–5.399, c = 7.088–7.162 Å, V = 175.5–180.8 Å^3. The smallest unit cell, with V = 175.5 Å^3, belongs to the holotype with the empirical formula $(Na_{1.92}K_{0.05}Ca_{0.02}Zn_{0.01})[S_{0.99}O_4]$ while the cotypes 2 and 1, with V = 178.0 and 180.8 Å^3, have the empirical formulae $(Na_{1.65}K_{0.11}Ca_{0.05}Cu_{0.04}Mg_{0.01})[S_{1.01}O_4]$ and $(Na_{1.54}K_{0.22}Ca_{0.09}Cu_{0.01}Mg_{0.01})[S_{1.00}O_4]$, respectively (Table 3). The content of the largest cation, K$^+$, seems to be the major cause of the increase in unit cell parameters.

The crystal structures of the different chemical varieties of metathénardite slightly differ from each other. In the crystal structure of cotype 2 the O(1) site is shifted more significantly from the m plane compared to cotype 1. In comparison with the holotype, both cotype specimens are enriched in K and bivalent cations, as well as vacancy defects. Such variable occupancy of Na(1) and Na(2) sites by components with different radii probably resulted in the irregular oxygen surroundings. This can cause the splitting of the O(1) site that increases the tetrahedral disorder.

Unlike thénardite, in which the SO$_4$ tetrahedra are regular with S–O = 1.48 Å (Hawthorne & Ferguson 1975), metathénardite contains distorted SO$_4$ tetrahedra and the degree of distortion depends on the content of admixed metal cations (and, probably, on the amount of vacancy defects caused by the presence of bivalent cations). The difference between the IR spectra of metathénardite and thénardite in the region of S–O stretching vibrations (see text above and Figure 6) reflects this structural difference.

For synthetic $Na_2SO_4(I)$, numerous isomorphous substitutions have been reported as well. Na$^+$ can be easily substituted by K$^+$ (Eysel 1973) or by bivalent (Ca, Sr, Ba, Pb, Mg, Mn, Co, Ni, Cu, Zn, Cd) and even trivalent (Cr, Fe, In, Y, Ln) metal cations (Eysel *et al.* 1985). The aliovalent substitutions, along with strong tetrahedral disorder, trigger the appearance of ionic conductivity of compounds isotypic to $Na_2SO_4(I)$
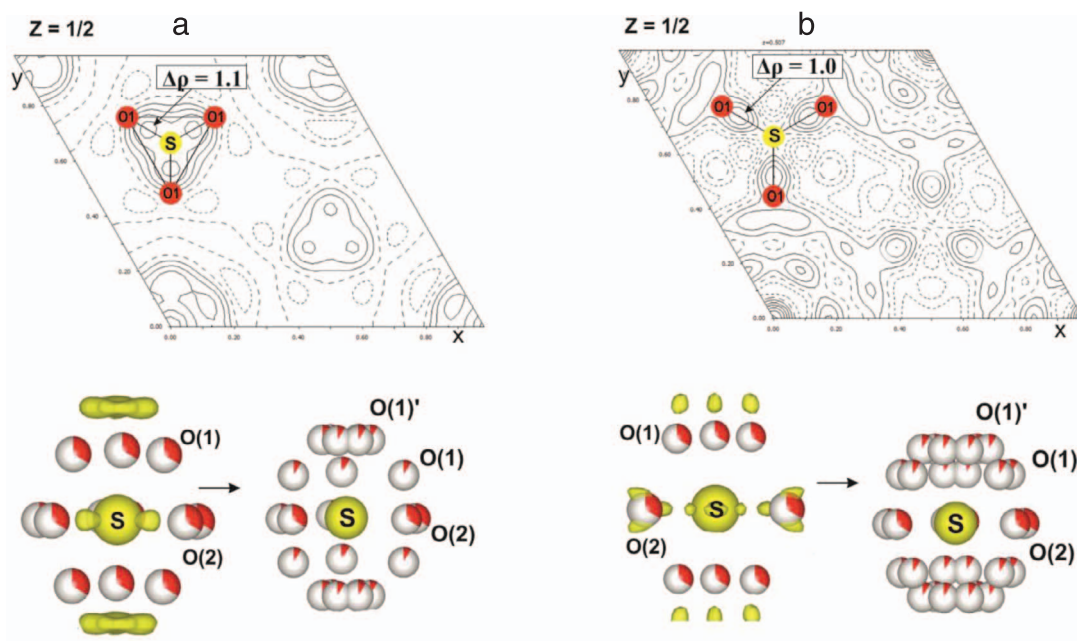
FIG. 8. Difference Fourier synthesis maps ($\triangle\rho xyz_{1/2}$) with maxima at the future O(1)' site, 3D-visualization of electron density maxima (yellow isosurfaces), and locations of O(1), O(1)', and O(2) atoms after splitting of the O(1) site: (a) cotype 1, (b) cotype 2. Occupation of the O sites is indicated in red. 3D-visualization of electron density maps was made using the VESTA program package (Momma & Izumi 2011). Solid lines on difference Fourier synthesis' maps outline the maxima of electron density and dashed lines outline the minima.

TABLE 4. ATOMIC COORDINATES AND CHARACTERISTICS OF SITES IN CRYSTAL STRUCTURE OF THE HOLOTYPE AND THE COTYPE SAMPLES OF METATHÉNARDITE

| Sample	Site	x/a	y/b	z/c	U_{eq}	Symmetry	Wyckoff symbol
Holotype	Na(1)				0.041(3)		
Cotype 1	Na(1)	0	0	0	0.035(1)	$\bar{3}m$	2a
Cotype 2	Na(1)				0.042(1)		
Holotype	Na(2)				0.089(6)		
Cotype 1	Na(2)	1/3	2/3	3/4	0.092(3)	$\bar{6}m2$	2d
Cotype 2	Na(2)				0.075(3)		
Holotype	S				0.035(2)		
Cotype 1	S	1/3	2/3	1/4	0.048(1)	$\bar{6}m2$	2c
Cotype 2	S				0.048(1)		
Holotype	O(1)	0.500(4)	0.750(4)	0.412(4)	0.15(2)	.m.	12k
Cotype 1	O(1)	0.596(5)	0.795(3)	0.367(3)	0.07(1)	1	24l
Cotype 1	O(1)'	0.415(4)	0.755(2)	0.459(3)	0.07(1)	1	24l
Cotype 2	O(1)	0.566(7)	0.743(6)	0.382(4)	0.09(1)	1	24l
Cotype 2	O(1)'	0.443(6)	0.646(4)	0.449(3)	0.09(1)	1	24l
Holotype	O(2)	0.224(9)	0.365(3)	1/4	0.03(1)	m..	12j
Cotype 1	O(2)	0.221(2)	0.370(1)	1/4	0.04(1)	m..	12j
Cotype 2	O(2)	0.150(9)	0.363(1)	1/4	0.05(1)	m..	12j
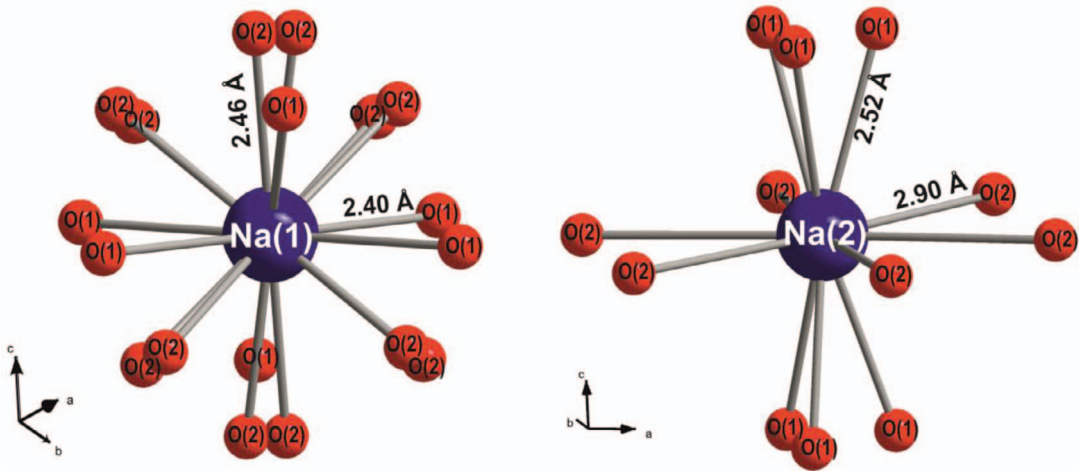
FIG. 9. Coordination spheres around sodium atoms at the Na(1) and Na(2) sites in the crystal structure of metathénardite (the holotype). Occupation of each O site is 1/3.

(Secco & Secco 1992, Secco & Usha 1994, and references therein). The conductivity of synthetic $Na_2SO_4(I)$, containing admixed bi- or trivalent cations and, correspondingly, vacancy defects, is due to the higher mobility of Na^+ in an expanded three-dimensional SO_4^{2-} sublattice. In such a crystal SO_4 tetrahedra are characterized by strong orientational disorder and Na^+ ions can move from vacancy to vacancy (Eysel et al. 1985).

The admixtures of bi- or trivalent metals widen the field of stability of $Na_2SO_4(I)$ to lower temperatures and stabilize its quenched form at room temperature

TABLE 5. COMPARATIVE DATA FOR METATHÉNARDITE,
ITS SYNTHETIC ANALOGUE $Na_2SO_4(I)$, AND THÉNARDITE

Mineral/Compound Ideal formula	Metathénardite Na_2SO_4	Synthetic $Na_2SO_4(I)$ Na_2SO_4	Thénardite Na_2SO_4
Crystal system	Hexagonal	Hexagonal	Orthorhombic
Space group	$P6_3/mmc$	$P6_3/mmc$	$Fddd$
a, Å	5.35–5.40	5.33–5.42	5.86–5.87
b, Å			12.30
c, Å	7.09–7.16	7.13–7.25	9.81–9.83
V, Å^3	175–181	175–184	707–710
Z	2	2	8
Strongest reflections	4.667–27	4.71–20	4.66–73
of the measured	3.904–89	3.94–100	3.178–51
powder X-ray	3.565–33	3.61–30	3.075–47
diffraction pattern:	2.824–94	2.865–90	2.783–100
d (Å) − I	2.686–100	2.703–90	2.646–48
	1.939–35	1.966–30	1.864–31
Optical data	Uniaxial	Not reported	Biaxial
α/ω	1.489		1.464–1.471
β			1.473–1.477
γ/ε	1.486		1.481–1.485
optical sign, 2V	(−)		(+) 83°
Source	This study	Fischmeister (1962), Eysel (1973), Eysel et al. (1985), Rasmussen et al. (1996)	Nord (1973), Hawthorne & Ferguson (1975), Mehrotra et al. (1978), Rasmussen et al. (1996), Anthony et al. (2003)

(Eysel *et al.* 1985). The Tolbachik samples were collected from hot areas of fumaroles with temperatures 350–400 °C where only the $Na_2SO_4(I)$ phase can exist. Metathénardite from both Glavnaya Tenoritovaya and Yadovitaya fumaroles and some samples from the Arsenatnaya fumarole remain stable after cooling, as no characteristic reflections of thénardite or other modifications of Na_2SO_4 have been detected in the powder XRD patterns not just a month after collecting but even after three years at room-standard conditions. The visual characteristics of such crystals also have not changed over time. These varieties of metathénardite contain admixtures of bivalent metals (Ca, Cu, Zn, Mg) (Tables 1 and 3) substituting for Na^+ that can explain their stability at room temperature.

Other crystals of metathénardite from Arsenatnaya that are chemically closer to the endmember changed under room conditions after several months or even several days. They lost transparency and became milky-white. Mechanisms and products of transformation of such samples will be described and discussed in the next paper in this series. The originally named metathénardite from fumaroles at Mt. Pelée volcano (Martinique), briefly reported by A. Lacroix as a presumably hexagonal high-temperature modification of Na_2SO_4, demonstrated similar behavior: its transparent crystals transformed to white opaque thénardite paramorphs soon after cooling (Lacroix 1910, Palache *et al.* 1951). Based on the above-discussed features of synthetic $Na_2SO_4(I)$, we can assume that the metathénardite of Lacroix, a hypothetical phase, was chemically almost pure Na_2SO_4 for which the formation of a quenched form seems hardly probable.

We assume that metathénardite can be a common constituent of relatively high-temperature ($>240–250$ °C) fumarole sublimates (*e.g.*, the presence of metathénardite was assumed in deposits of hot fumaroles at the Eldfell volcano, Iceland; Mitolo *et al.* 2008), but probably only the Me^{2+}/Me^{3+}-bearing varieties of the mineral have a chance to "survive" after cooling.

References

ANTHONY, J.W., BIDEAUX, R.A., BLADH, K.W., & NICHOLS, M.C. (2003) *Handbook of Mineralogy. V. Borates, Carbonates, Sulfates*. Mineral Data Publishing, Tucson, Arizona.

BELLANCA, A. (1942) L'aftitalite nel Sistema ternario K_2SO_4–Na_2SO_4–$CaSO_4$. *Periodico di Mineralogia* **13**, 21–86.

BERG, A.J. & TUNISTRA, F. (1978) The space group and structure of α-K_2SO_4. *Acta Crystallographica* **B34**, 3177–3181.

CHUKANOV, N.V., AKSENOV, S.M., RASTSVETAEVA, R.K., PEKOV, I.V., BELAKOVSKI, D.I., & BRITVIN, S.N. (2015) Möhnite, $(NH_4)K_2Na(SO_4)_2$, a new guano mineral from Pabellon de Pica, Chile. *Mineralogy and Petrology* **109**, 643–648.

CODY, C.A., DICARLO, R., & DARLINGTON, R.K. (1981) Differential scanning calorimetric and Raman spectroscopic study of polymorphism in Na_2SO_4. *Journal of Inorganic and Nuclear Chemistry* **43**, 398–400.

DESSUREAULT, Y., SANGSTER, J., & PELTON, A.D. (1990) Coupled phase diagram/thermodynamic analysis of the nine common-ion binary system involving the carbonates and sulfates of lithium, sodium and potassium. *Journal of Electrochemical Society* **137(9)**, 2941–2950.

DU, H. (2000) Thermodynamic assessment of the K_2SO_4–Na_2SO_4–$MgSO_4$–$CaSO_4$ system. *Journal of Phase Equilibria* **21(1)**, 6–18.

EYSEL, W. (1970) Strukturen und Umwandlungen von Mischkristallen in System Na_2SO_4–K_2SO_4. *Zeitschrift für Kristallographie* **132**, 426–427.

EYSEL, W. (1972) DTA and DSC of compounds and solid solutions in the system Na_2SO_4–K_2SO_4. Proceedings of the third International Conference on Thermal Analysis, Davos, Switzerland, 179–192.

EYSEL, W. (1973) Crystal chemistry of the system Na_2SO_4–K_2SO_4–K_2CrO_4–Na_2CrO_4 and of the glaserite phase. *American Mineralogist* **58**, 736–747.

EYSEL, W., HOEFER, H.H., KEESTER, K.L., & HAHN, T. (1985) Crystal chemistry and structure of $Na_2SO_4(I)$ and its solid solutions. *Acta Crystallographica* **B41**, 5–11.

FEDOTOV, S.A. & MARKHININ, Y.K., Eds. (1983) *The Great Tolbachik Fissure Eruption*. Cambridge University Press, New York City, New York, United States.

FILATOV, S.K., SHABLINSKII, A.P., VERGASOVA, L.P., SAPRIKINA, O.Y., BUBNOVA, R.S., MOSKALEVA, S.V., & BELOUSOV, A.B. (2019) Belomarinaite $KNa(SO_4)$: A new sulphate from 2012–2013 Tolbachik Fissure Eruption, Kamchatka Peninsula, Russia. *Mineralogical Magazine* **83**, 569–575.

FISCHMEISTER, H.F. (1962) Röntgenkristallographische Ausdehnungsmessungen an einigen Alkalisulfaten. *Monatshefte für Chemie* **93**, 420–434.

GORELOVA, L.A., VERGASOVA, L.P., KRIVOVICHEV, S.V., AVDONTSEVA, E.YU., MOSKALEVA, S.V., KARPOV, G.A., & FILATOV, S.K. (2016) Bubnovaite, $K_2Na_8Ca(SO_4)_6$, a new mineral species with modular structure from the Tolbachik volcano, Kamchatka peninsula, Russia. *European Journal of Mineralogy* **28**, 677–686.

GOSSNER, B. (1928) Über die Kristallstruktur von Glaserit und Kaliumsulfat. *Neues Jahrbuch für Mineralogie, Geologie und Palaeontologie* **57A**, 89–116.

HAWTHORNE, F.C. & FERGUSON, R.B. (1975) Anhydrous sulphates. I. Refinement of the crystal structure of celestite with an appendix on the structure of thenardite. *Canadian Mineralogist* **13**, 181–187.

HILMY, M.E. (1953) Structural crystallographic relation between sodium sulfate and potassium sulfate and some other synthetic sulfate minerals. *American Mineralogist* **38**, 118–135.

KRACEK, F.C. & KSANDA, C.J. (1930) Polymorphism of sodium sulfate: IV. X-Ray analysis. *Journal of Physics and Chemistry* **34**, 1741–1744.

KUMARI, M.S. & SECCO, E. (1983) Order-disorder transitions and solid-state reaction kinetics in $Na_2SO_4–K_2SO_4$ system. *Canadian Journal of Chemistry* **61**, 594–598.

LACROIX, A. (1910) *Minéralogie de la France* (t. IV). Librairie Polytechnique, Paris, France.

LAZORYAK, B.I. (1996) Design of inorganic compounds with tetrahedral anions. *Russian Chemical Reviews* **65(4)**, 287–305.

MANDARINO, J.A. (1981) The Gladstone-Dale relationship. Part IV. The compatibility concept and its application. *Canadian Mineralogist* **14**, 498–502.

MEHROTRA, B.N., HAHN, T., EYSEL, W., ROEPKE, H., & ILLGUTH, A. (1978) Crystal chemistry of compounds with thenardite (Na_2SO_4 V) structure. *Neues Jahrbuch für Mineralogie Monatshefte*, 408–421.

MITOLO, D., GARAVELLI, A., PEDERSEN, L., BALIĆ-ŽUNIĆ, T., JAKOBSSON, S.P., & VURRO, F. (2008) Mineralogy of actually forming sublimates at Eldfell Volcano, Heimaey (Vestmannaeyjar archipelago), Iceland. *Plinius* **34**, 322.

MIYAKE, M., MORIKAWA, H., & IWAI, S. (1980) Structure reinvestigation of the high-temperature form of K_2SO_4. *Acta Crystallographica* **B36**, 532–536.

MOMMA, K. & IZUMI, F. (2011) VESTA 3 for three-dimensional visualization of crystal, volumetric and morphology data. *Journal of Applied Crystallography* **44**, 1272–1276.

MOORE, P.B. (1973) Bracelets and Pinwheels: a topological-geometrical approach to the calcium orthosilicate and alkali sulfate structures. *American Mineralogist* **58**, 32–42.

MOORE, P.B. (1976) The glaserite, $K_3Na[SO_4]_2$, structure type as a super dense-packed oxide: evidence for icosahedral geometry and cation-anion mixed layer packings. *Neues Jahrbuch für Mineralogie Abhandlungen* **127(2)**, 187–196.

MOORE, P.B. (1981) Complex crystal structures related to glaserite, $K_3Na[SO_4]_2$: Evidence for very dense packings among oxysalts. *Bulletin of Mineralogy* **104(4)**, 536–547.

NAKAMOTO, K. (1986) *Infrared and Raman Spectra of Inorganic and Coordination Compounds*. John Wiley & Sons, New York, United States.

NARUSE, H., TANAKA, K., MORIKAWA, H., MARUMO, F., & MEHROTRA, B.N. (1987) Structure of Na_2SO_4 at 693 K. *Acta Crystallographica* **B43**, 143–146.

NIKOLOVA, R. & KOSTOV-KYTIN, V. (2013) Crystal chemistry of "glaserite" type compounds. *Bulgarian Chemical Communications* **45(4)**, 418–426.

NORD, A.G. (1973) Refinement of the crystal structure of thenardite, Na_2SO_4(V). *Acta Chemica Scandinavica* **27**, 814–822.

OKADA, K. & OSSAKA, J. (1980) Structures of potassium sodium sulphate and tripotassium sodium disulphate. *Acta Crystallographica* **B36**, 919–921.

PALACHE, C., BERMAN, H., & FRONDEL, C. (1951) *Dana's System of Mineralogy*. 7th Edition, Vol. II, p. 407.

PEKOV, I.V., ZUBKOVA, N.V., BELAKOVSKIY, D.I., LYKOVA, I.S., YAPASKURT, V.O., VIGASINA, M.F., SIDOROV, E.G., & PUSHCHAROVSKY, D.YU. (2015) Sanguite, $KCuCl_3$, a new mineral from the Tolbachik volcano, Kamchatka, Russia. *Canadian Mineralogist* **53**, 633–641.

PEKOV, I.V., GURZHIY, V.V., ZUBKOVA, N.V., AGAKHANOV, A.A., BELAKOVSKIY, D.I., VIGASINA, M.F., & SIDOROV, E.G. (2016) Metathénardite, IMA 2015-102. CNMNC Newsletter No. 30, April 2016, p. 408. *Mineralogical Magazine* **80**, 407–413.

PEKOV, I.V., KOSHLYAKOVA, N.N., ZUBKOVA, N.V., LYKOVA, I.S., BRITVIN, S.N., YAPASKURT, V.O., AGAKHANOV, A.A., SHCHIPALKINA, N.V., TURCHKOVA, A.G., & SIDOROV, E.G. (2018) Fumarolic arsenates – a special type of arsenic mineralization. *European Journal of Mineralogy* **30**, 305–322.

PETŘÍČEK, V., DUŠEK, M., & PALATINUS, L. (2014) Crystallographic Computing System JANA2006: General features. *Zeitschrift für Kristallographie* **229(5)**, 345–352.

RASMUSSEN, S.E., JORGENSEN, J.E., & LUNDTOFT, B. (1996) Structures and phase transitions of Na_2SO_4. *Journal of Applied Crystallography* **29**, 42–47.

SECCO, R.A. & SECCO, E.A. (1992) Effect of pressure on the electrical conductivity, Na^+-ion transport, in Na_2SO_4. *Chemistry of Solids* **53(6)**, 749–753.

SECCO, E.A. & USHA, M.G. (1994) Cation conductivity in mixed sulfate-based composition of Na_2SO_4, Ag_2SO_4, and Li_2SO_4. *Solid State Ionics* **68**, 213–219.

SHCHIPALKINA, N.V., PEKOV, I.V., CHUKANOV, N.V., ZUBKOVA, N.V., BELAKOVSKIY, D.I., KOSHLYAKOVA, N.N., BRITVIN, S.N., SIDOROV, E.G., & VOZCHIKOVA, S.A. (2018) Natroaphthitalite, IMA 2018-091. CNMNC Newsletter No. 46, December 2018, p. 1185. *European Journal of Mineralogy* **30**, 1181–1189.

SHELDRICK, G.M. (2007) *SADABS*. University of Göttingen, Göttingen, Germany.

SMITHSON, J. (1813) On a saline substance from Mount Vesuvius. *Royal Society of London Philosophical Transactions*, 256–262.

VERGASOVA, L.P. & FILATOV, S.K. (2016) A study of volcanogenic exhalation mineralization. *Journal of Volcanology and Seismology* **10(2)**, 71–85.

ZUBKOVA, N.V., PEKOV, I.V., KSENOFONTOV, D.A., YAPASKURT, V.O., PUSHCHAROVSKY, D.YU., & SIDOROV, E.G. (2018) Arcanite from fumarole exhalations of the Tolbachik volcano (Kamchatka, Russia) and its crystal structure. *Doklady Earth Sciences* **479(1)**, 339–341.